Hindawi
Security and Communication Networks
Volume 2023, Article ID 9894101, 1 page
https://doi.org/10.1155/2023/9894101

Retraction

Retracted: Adaptive Control Strategy of Multiemergency Power Supply Network System Connected to New Energy

Security and Communication Networks

Received 26 December 2023; Accepted 26 December 2023; Published 29 December 2023

This article has been retracted by Hindawi, as publisher, following an investigation undertaken by the publisher [1]. This investigation has uncovered evidence of systematic manipulation of the publication and peer-review process. We cannot, therefore, vouch for the reliability or integrity of this article.

Please note that this notice is intended solely to alert readers that the peer-review process of this article has been compromised.

Wiley and Hindawi regret that the usual quality checks did not identify these issues before publication and have since put additional measures in place to safeguard research integrity.

We wish to credit our Research Integrity and Research Publishing teams and anonymous and named external researchers and research integrity experts for contributing to this investigation.

The corresponding author, as the representative of all authors, has been given the opportunity to register their agreement or disagreement to this retraction. We have kept a record of any response received.

References

[1] W. Zhang, M. Zhong, M. A, Y. Sun, and Y. Wang, "Adaptive Control Strategy of Multiemergency Power Supply Network System Connected to New Energy," *Security and Communication Networks*, vol. 2022, Article ID 5733358, 11 pages, 2022.

Hindawi
Security and Communication Networks
Volume 2022, Article ID 5733358, 11 pages
https://doi.org/10.1155/2022/5733358

Research Article

Adaptive Control Strategy of Multiemergency Power Supply Network System Connected to New Energy

Wei Zhang,[1,2,3] **Ming Zhong**,[2,3] **Minfu A**,[2,3] **Yumei Sun**,[4] **and Yang Wang**[4]

[1]*Polytechnic Institute, Zhejiang University, Hangzhou, Zhejiang 310015, China*
[2]*Inner Mongolia Power Research Institute, Hohhot, Inner Mongolia 010020, China*
[3]*Inner Mongolia Enterprise Key Laboratory of Smart Grid Simulation of Electrical Power System, Hohhot, Inner Mongolia 010020, China*
[4]*Inner Mongolia Borelles Electric Power Engineering Design Co., Ltd., Hohhot, Inner Mongolia 010010, China*

Correspondence should be addressed to Wei Zhang; 11810089@zju.edu.cn

Received 17 June 2022; Revised 2 August 2022; Accepted 27 August 2022; Published 15 September 2022

Academic Editor: Tao Cui

In order to improve the adaptive control effect of the multiemergency power supply networking system connected to new energy (NE), this paper studies the adaptive control strategy (ACS) of the multiemergency power supply networking system connected to NE by combining intelligent algorithms and determines the appropriate installation node of the distributed power supply according to the voltage stability index. Moreover, this paper proposes a method to optimize the distribution network feeder reorganization and distributed power configuration problems based on the fireworks algorithm to reduce the network loss and improve the voltage distribution. In addition, distribution network reorganization and distributed power configuration optimization can more effectively minimize network losses and improve voltage distribution. Through the experimental research, it can be seen that the ACS of the multiemergency power supply network system connected to NE proposed in this paper has the established effect.

1. Introduction

As the common carrier of power transmission and power market, the power grid is the basic platform and main medium to ensure the development of NE [1]. Therefore, regional power grids are an inherent requirement and an inevitable choice to transform the energy structure and power development mode and achieve sustainable development [2] such as uncoordinated planning and construction, lack of management of power generation and grid-connected operation, inadequate technical standards, approval of supporting grid projects, and approval and construction lag to accurately and deeply recognize these problems [3]. Under such a background, it is urgent to build a comprehensive evaluation index system and corresponding evaluation methods that can reflect the coordinated development (CD) of NE and regional power grids, so as to enhance the identification of the degree of development coordination between the two. The results of the study found the key influencing factors of the CD, and provided a reference for the relevant departments to formulate the promotion measures for the CD of the two [4]. In addition, there are still many problems in the current electricity market system, such as the competition mechanism only exists on the power generation side, and the electricity price mechanism cannot meet the market demand. This requires the establishment and improvement of a power supervision mechanism that adapts to the market structure to optimize power generation side management, power transmission and distribution management, and power sales side management [5]. Under the premise that the scale of NE power generation (NEPG) and grid connection is expanding, a comprehensive evaluation system and method for the development of NE and regional power grids should be constructed, and the problems existing in the power generation management end and power supply management

end should be found in time, which is conducive to the effective use of resources and energy. The optimal configuration in space can promote the power system to meet the various requirements of the market and the environment, and improve social welfare [6]. Since large-scale NEPG has been developed in recent years, its coordinated planning with regional power grids belongs to an emerging power development model. At present, there are relatively few studies on the coordination evaluation method of this model [7].

The literature [8] is based on AHP-distance. The coordination degree combination model conducts a comprehensive evaluation and research on the coordination degree of low-carbon power grid planning. Reference [9] analyzes the coordination degree between distribution network and power load from the aspects of reliability of power supply, equipment utilization, and characteristics of economic operation. Based on the analysis of the three aspects of safety, reliability, and economy, the literature [10] pointed out that photovoltaic power generation has an impact on the traditional power grid. Therefore, an index system reflecting the CD of photovoltaic power generation and power grid has been constructed. Combined with the connotation of CD, a set of comprehensive evaluation index system that can reflect the CD of NE and regional power grids is constructed by defining and analyzing the coordinated planning mode of NE sources and regional power grids. The corresponding weights are constructed from the comprehensive evaluation model [11] and using this model to evaluate the CD degree of NE and regional power grids in the whole country [12] and draw relevant conclusions, in order to provide decision-making reference for the coordinated planning of NE and regional power grids [13].

Power sources can be divided into traditional power sources and NE sources according to the type of energy. The power source formed by traditional power generation methods such as thermal power generation and hydropower generation is the traditional power source. According to the voltage level of the transmission line, the power grid can be divided into transmission network and distribution network [14]. The operation of the power system includes power generation, transmission and distribution, dispatching, and electricity consumption. Therefore, the CD of NE and regional power grids requires manpower from four links. Among them, the coordination of NEPG is the basic link that affects the coordination degree of the entire regional power grid, power transmission, and distribution includes transmission, distribution, and transmission. It is an important link of large-scale development [15]; dispatching is the control and monitoring link of the entire power system and the realization of intelligent dispatching of regional power grids is an important guarantee for effectively realizing the CD of NEPG and regional power grids. Electricity consumption is an important part of the entire power system. The friendly and interactive power consumption link is conducive to the entire power system to quickly grasp the dynamic changes of NEPG [16]. It is necessary to realize the CD of the power supply at the power generation end and the power grid at the transmission end in all aspects, so as to achieve the goal of ultimately achieving the overall CD of the power supply and the power grid. It is necessary to comprehensively consider the evaluation indicators of the mutual coordination and development of the four subsystems, including power generation, transmission and distribution, dispatching, and power consumption [17].

When the small-capacity NE power source is connected to the unbalanced distribution network, if the short-circuit calculation is still based on the traditional symmetrical component method after improvement, the power components will be difficult to decouple under the conditions of positive, negative, and zero sequence, and the calculation result will have a big difference from the actual results, that is, the improved symmetrical component calculation method makes it difficult to perform fault calculation for the unbalanced distribution network with different types of NE power sources. Therefore, it is necessary to carry out research on new short-circuit calculation methods for different types of NE sources connected to unbalanced distribution networks.

The contribution of this paper is to analyze the ACS of multiple NE access multiemergency power supply networking systems such as island detection. In traditional research, only one of these methods is often considered as the optimization object, but this paper adopts both optimization methods. The power distribution system integrated with NE is optimized by means of this method, and simulation research is carried out according to different planning situations.

2. Grid Adaptive Control

2.1. Radial Islanding Detection in Distribution Network. For the normal operation of the radial distribution network, the situation of ring network and island operation should be avoided. This paper starts from the following three aspects to ensure that the topological structure of the system after the feeder reorganization can meet all the loads connected to the system, and the distribution network operates radially [18]:

(1) Detection procedures for ring networks and islands;

(2) Breadth-first node number generation;

(3) "Pseudoring network" processing based on tie switch.

Whether it is to detect the ring network or the island, it is necessary to form the adjacency matrix of the topology structure of the power distribution system, and the adjacency matrix form required for different researches is also different. This paper uses the node-node adjacency matrix, and the two adjacent nodes are set to 1, otherwise it is set to 0.

2.1.1. Ring Network Detection. It takes the upper triangular matrix of the adjacency matrix, the number of nonzero values of the upper triangular matrix is the number of branches of the network, and the value minus the number of network nodes plus 1 equals the number of rings in the network.

2.1.2. Island Detection. Island detection is to detect the connectivity of the system. According to the adjacency matrix of the network, all connected nodes are searched from the first node (usually a transformer station), and it is judged that these nodes form continuous branches, respectively. In this way, the row vector of the final result matrix represents the continuous branches in the network, and the column vector represents the node number contained in each branch. That is, if the system has no islands, the result matrix is in the form of $1 \times n$, where n is the number of network nodes.

For different networks, the node numbering forms in the network data are often not uniform, and it is obviously unrealistic to manually organize the system network node and branch data into a uniform format. The most important thing is that the topological structure of the network after the optimization of the feeder reorganization will change, so it is particularly important to intelligently optimize the numbering of any structure that appears in the feeder reorganization.

This paper adopts the form of breadth-first node numbering. Numbering nodes in this way can ensure that the network formed by the included nodes is radiative and avoids the appearance of ring networks and isolated islands.

We assume that the network structure is shown in Figure 1, and the breadth-first node numbering process is as follows:

Step 1: as shown in Figure 1, the node number in the circle is the initial node, the first node is the substation node, which is set to No. 1, and its child node is set to No. 2 (for example, the initial node No. 6 is changed to No. 2), and the rest of the node numbers remain unchanged for the time being and are still any previous values.

Step 2: the algorithm searches for the branch connected to branch 1. If the parent node of one of the branches is the child node of the new label of the previous branch, for example, the parent nodes of branch 2 and branch 3 are the child nodes of branch 1, node 2, the order of nodes 3 and 4 is in the order of the branch label from low to high, then the child nodes of branch 2 and branch 3 are renumbered as 3 and 4, respectively.

Step 3: the algorithm searches again for the branch connected to the new numbered node 3. Since there is no branch connected to it, the branch connected to the newly numbered node 4 is searched instead. Branch 4 and branch 7 are connected to this node, so the parent node of the branch 4 and the branch 7 is 4, and the child nodes are 5 and 6, respectively.

2.2. "Pseudoring" Partition Based on Tie Switch. This paper defines "pseudoring network" as a ring network composed of tie switches and branches as shown in Figure 2. Figure 2 is the structure diagram of the IEEE-33 node test system. The system has five tie switches, which can form a ring network Lp1-Lp5 according to the form in the figure. Moreover, the branches not included in the ring network do not participate

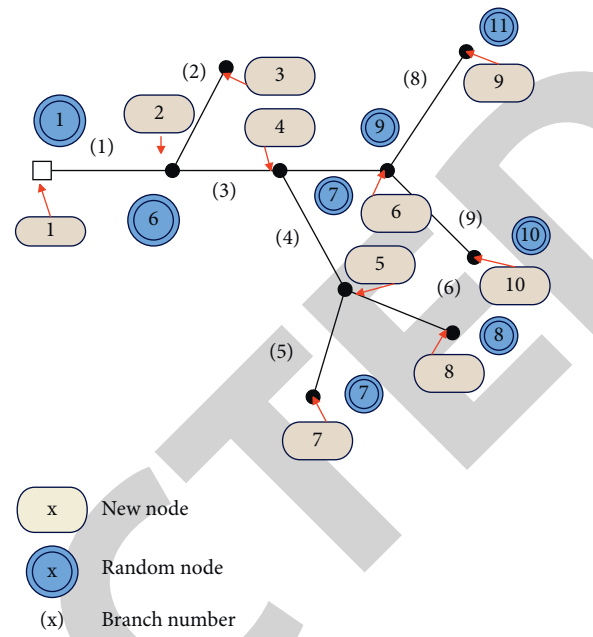

Figure 1: Example of node labeling.

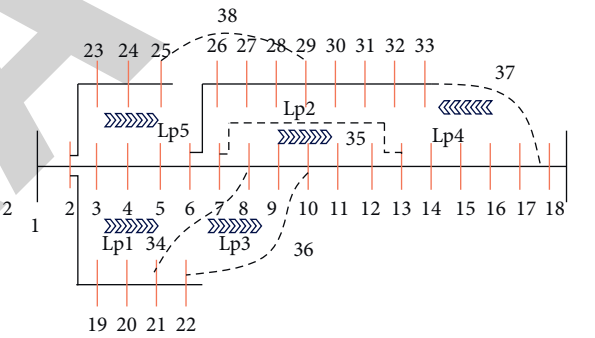

Figure 2: Pseudoring network topology of IEEE-33 node system.

in the process of feeder reorganization optimization. Because in a separate branch, if a segment switch is disconnected, an island node will inevitably be generated, so only the branch covered by the ring network is used as the range to be optimized. When the feeder is reorganized, only one switch in each loop can be opened.

The advantages of the ring network coding method are described below by taking a 33 node test system as an example. If the segment switch is considered a branch, there are a total of 37 branches in the system. According to the traditional optimization method, each optimized position (gene locus) is a 0/1 state quantity. In this method, the number of branches contained in each loop is 7, 10, 11, 7, and 16, respectively. It is easy to obtain them. The product of 86240, the computational burden is significantly reduced. In addition, compared with the traversal method, the use of this coding method itself can greatly reduce the possibility that the generated network topology structure contains ring network or island nodes. If combined with the ring network and island detection procedures, the generated topology can conform to the radial structure without islands.

2.3. Voltage Stability Index. The voltage stability index is used to "preset" the access nodes of the distributed power generation. Its functions are as follows:

(1) The voltage distribution is one of the optimization goals of this chapter, and the voltage stability of each node is evaluated using the voltage stability index proposed in the literature. Moreover, nodes with lower stability indicators are more prone to voltage collapse.

Therefore, the voltage stability indicators of each node are calculated, and the indicators are arranged from low to high, and they are used as the optimal access nodes for distributed power sources. If there are three distributed power sources, the three nodes with the smallest voltage stability indicators are selected.

(2) The location selection of access nodes, both of which are regarded as variables to be optimized in traditional methods. Before optimization, "presetting" the access node can effectively reduce the search space of the optimization algorithm.

Figure 3 is a schematic diagram of a simple power flow through the feeder. The problem is simplified as follows:

The impedance of the line is $R_k + jX_k$, the load between node k and node $k+1$ is $P_{k+1} + Q_{k+1}$, and the formula can be written from Figure 3:

$$I_k = \frac{V_k - V_{k+1}}{R_k + jX_k}, \tag{1}$$

$$P_{k+1} - jQ_{k+1} = V_{k+1} \cdot I_k. \tag{2}$$

Among them, k represents the branch number or starting node number, represents the current of branch k, V_k/V_{k+1} represents the voltage ratio between node k and node $k+1$, and P_{k+1}/Q_{k+1} represents the active and reactive power transmitted from the feeder to node $k+1$.

From formulas (1) and (2), we get

$$\begin{aligned} &\left|V_{k+1}\right| - \left\{\left|V_k\right| - 2P_{k+1}r_k - 2Q_{k+1}x_k\right\}\left|V_{k+1}\right|^2 \\ &+ \left\{P_{k+1}^2 + Q_{k+1}^2\right\}\left\{r_k^2 + x_k^2\right\} = 0. \end{aligned} \tag{3}$$

We assume the following:

$$\begin{aligned} b_k &= \left|V_k\right| - 2P_{k+1}r_k - 2Q_{k+1}x_k, \\ c_k &= \left\{P_{k+1}^2 + Q_{k+1}^2\right\}\left\{r_k^2 + x_k^2\right\}. \end{aligned} \tag{4}$$

Formula (3) is simplified to

$$\left|V_{k+1}\right| - b_k\left|V_{k+1}\right|^2 + c_k = 0. \tag{5}$$

From formula (5), it can be seen that the solution of $|V_{k+1}|$ has the following four cases:

(1) $0.707\left[b_k - \left\{b_k^2 - 4c_k\right\}^{1/2}\right]^{1/2}$

(2) $-0.707\left[b_k - \left\{b_k^2 - 4c_k\right\}^{1/2}\right]^{1/2}$

(3) $-0.707\left[b_k + \left\{b_k^2 - 4c_k\right\}^{1/2}\right]^{1/2}$

(4) $0.707\left[b_k + \left\{b_k^2 - 4c_k\right\}^{1/2}\right]^{1/2}$

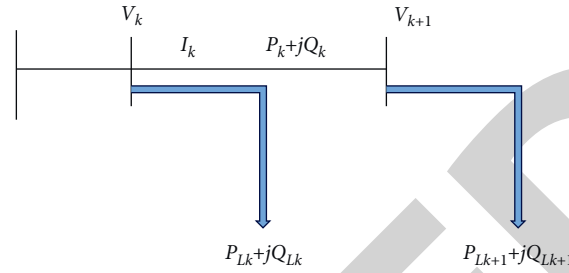

Figure 3: Schematic diagram of feeder.

According to the real data, P, Q, r, x, and V are generally expressed in the form of per-unit values, and b_k is usually positive. Since the ratio of $2P_{k+1}r_k + 2Q_{k+1}x_k$ and $|V_k|^2$ is usually small, the value of $4c_k$ is also small relative to b_k^2, so $\left\{b_k^2 - 4c_k\right\}^{1/2}$ is approximately equal to b_k. Then, the values of the results (1) and (2) of $|V_{k+1}|$ are close to 0, which is not suitable, the value of the result (3) is negative, and the value of the result (4) is positive and practical. Therefore, the value of equation (5) is uniquely determined and its value is as follows:

$$\left|V_{k+1}\right| = 0.707\left[b_k + \left\{b_k^2 - 4c_k\right\}^{1/2}\right]^{1/2}. \tag{6}$$

From formula (6), it can be seen that the conditions for the existence of the power flow calculation solution of the radial distribution system are as follows:

$$\begin{aligned} &b_k^2 - 4c_k \geq 0, \\ &\left\{\left|V_k\right|^2 - 2P_{k+1}r_k - 2Q_{k+1}x_k\right\}^2 + 4.0\left\{P_{k+1}^2 + Q_{k+1}^2\right\}\left\{r_k^2 + x_k^2\right\} \geq 0. \end{aligned} \tag{7}$$

After simplification,

$$\begin{aligned} &\left|V_k\right|^4 - 4.0\left\{P_{k+1}x_k - Q_{k+1}r_k\right\}^2 \\ &\quad - 4.0\left\{P_{k+1}r_k + Q_{k+1}x_k\right\}\left|V_k\right|^2 \geq 0. \end{aligned} \tag{8}$$

We get

$$\begin{aligned} VSI_{k+1} = &\left|V_k\right|^4 - 4.0\left\{P_{k+1}x_k - Q_{k+1}r_k\right\}^2 \\ &- 4.0\left\{P_{k+1}r_k + Q_{k+1}x_k\right\}\left|V_k\right|^2. \end{aligned} \tag{9}$$

Among them, VSI_{k+1} is the voltage stability index of node $k+1$. Its value represents the stability level of the radial distribution network. The fireworks algorithm is used to solve the problems of distribution network feeder reorganization and distributed power configuration.

As mentioned earlier, this paper uses voltage stability as the basis for which node the distributed power source is connected to, and the configuration capacity is determined by the optimization result of the fireworks algorithm.

2.4. Mathematical Model of Feeder Reorganization in Distribution Network

2.4.1. Optimization Objective

(1) System Network Loss. The mathematical model of power flow calculation will not be repeated in this chapter. The

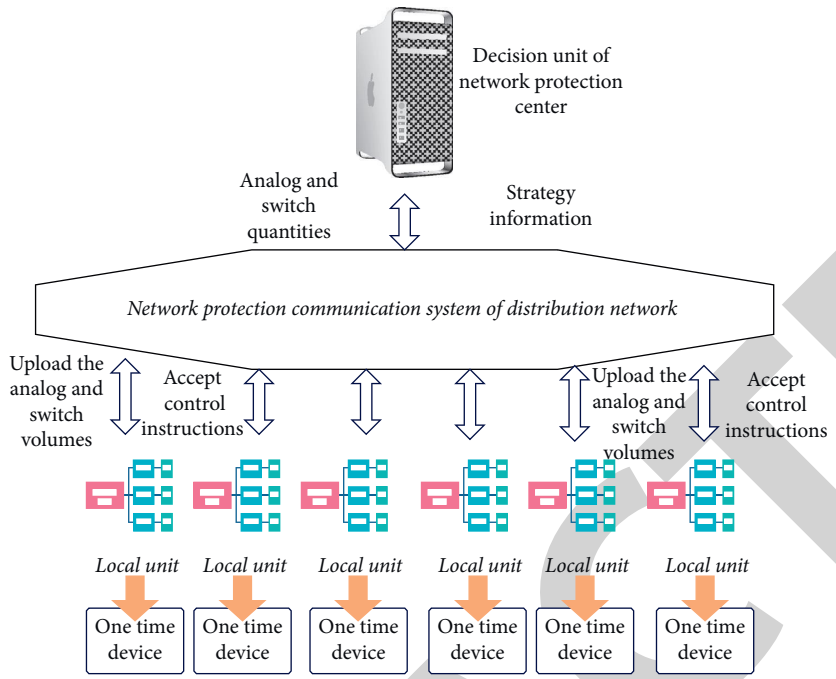

Figure 4: Schematic diagram of the networked protection system of the distribution network.

network loss of each branch of the distribution network is obtained through a power flow calculation as shown in the following formula.

$$P_{\text{Loss}}(k, k+1) = R_k \times \left(\frac{P_k^2 + Q_k^2}{|V_k|^2} \right), \tag{10}$$

$$P_{T,\text{Loss}} = \sum_{k=1}^{nb} P_{\text{Loss}}(k, k+1). \tag{11}$$

Among them, nb is the total number of branches of the system.

(2) Voltage Offset Index. A significant benefit that should be brought about by optimizing the network structure and distributed power configuration is that it can reduce the offset of the voltage of each node. The purpose of the voltage offset index is to prevent the capacity or layout of the distributed power supply from causing excessive voltage offset to the distribution system. The voltage offset index △VD is defined as follows:

$$\triangle V_D = \max\left(\frac{V_1 - V_2}{V_1} \right). \tag{12}$$

Combining the above two points, the optimization objective function is as follows:

$$F = \min\left[\left(\frac{P_{T,\text{Loss}}^{op}}{P_{T,\text{Loss}}} + \Delta V_D = \right) \right]. \tag{13}$$

Among them, $P_{T,\text{Loss}}^{op}$ is the optimized system network loss, and $P_{T,\text{Loss}}$ is the initial network loss of the system.

2.4.2. Constraints. (1) Power limitation:

$$P_{\text{sub}} = \sum_{k=2}^{n} P_{LK} + \sum_{k=2}^{n} P_{\text{Loss}}(k, k+1) - \sum_{k=2}^{n} P_{DG,k}. \tag{14}$$

(2) Voltage offset limitation:

$$|V_1 - V_k| \le \Delta V_{\max}. \tag{15}$$

(3) Feeder capacity limitation:

$$|S_k| \le |S_{k,\max}|. \tag{16}$$

(4) Distributed power capacity limitation:

$$P_{T\,DG}^{\min} \le P_{T\,DG} \le P_{T\,DG}^{\max}. \tag{17}$$

Among them, $P_{T\,DG}^{\min} = 0.1 \times \sum_{k=2}^{n} P_{LK}$, and $P_{T\,DG}^{\max} = 0.6 \times \sum_{k=2}^{n} P_{LK}$.

(5) Radial structure limitation:

$$N_L = N_{br} - N_{\text{bus}} + 1. \tag{18}$$

N_L is 0, which means that the system topology after the feeder reorganization has no ring network. In the optimization process, if any point of the above constraints is violated, the optimization result is invalid.

2.5. Optimization Process Based on Fireworks Algorithm. This section introduces how to apply the evolutionary algorithm to the optimization of the distribution network, such as the selection of the number of fireworks, and the

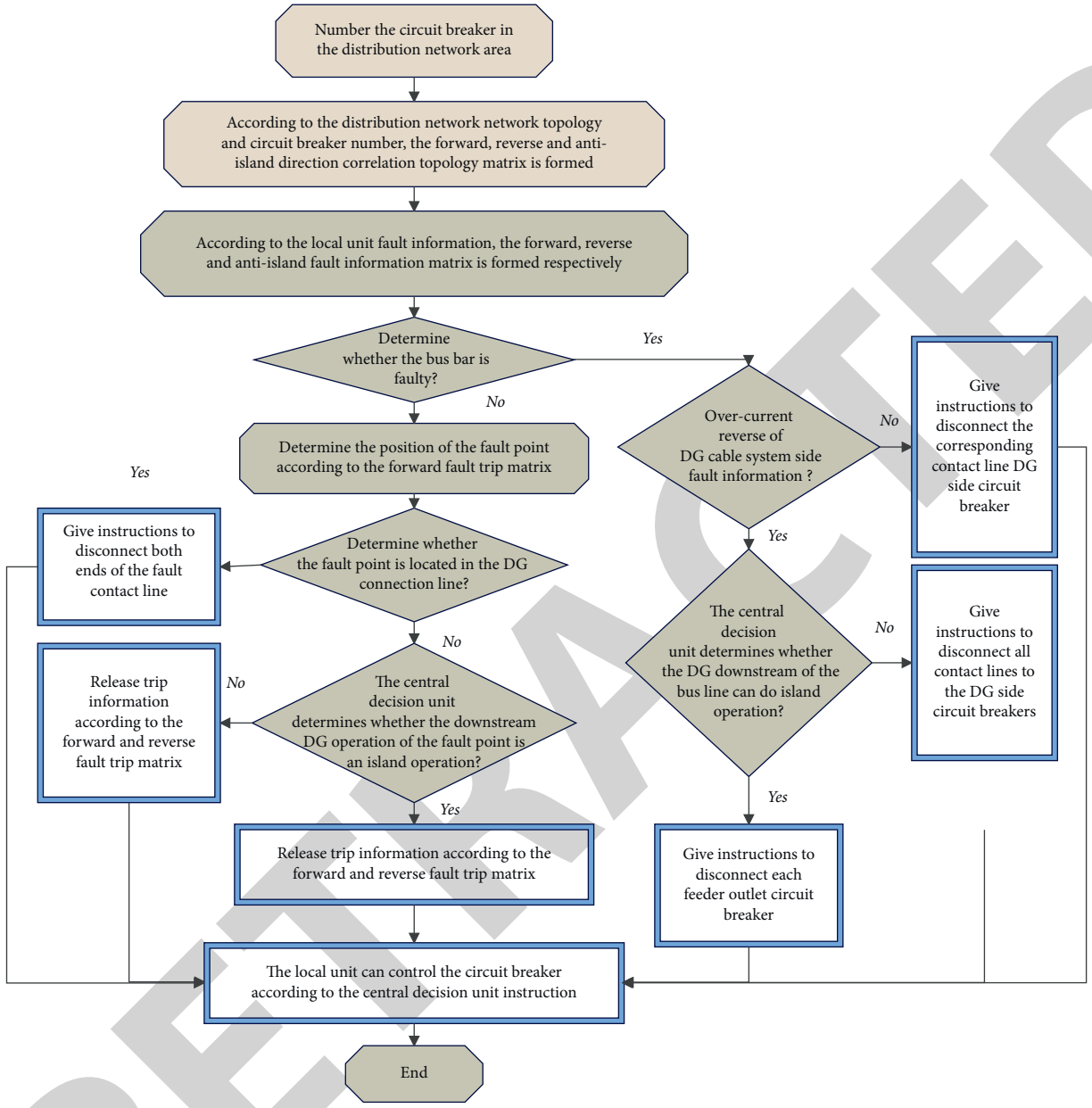

Figure 5: Principle of networked protection of distribution network connected to NE.

setting of each firework bit (gene bit). The main steps of applying fireworks algorithm to optimize distribution network structure and distributed power configuration are as follows:

Step 1: initializing fireworks algorithm parameters

(1) N: the number of iterations of the algorithm, and in this section $N = 50$ is selected.
(2) d: the dimension of the search space. This section should be set to the number of switches and distributed power sources for each "pseudoring network" partition described in Section 3. Here, it is set to 3, then the total problem dimension is $d = 5 + 3$.
(3) n: the number of fireworks, and it is set to $n = 20$.
(4) m: control variable for the total number of sparks.
(5) A: maximum explosion radius.
(6) Constants $s_{\min} = \text{round}(x\ m)$ and $S_{\max} = \text{round}(y\ m)$, where $x = 0.08$ and $y = 0.8$. Finally, the rounding operation is performed on $s_{\min}$ and $s_{\max}$.

Step 2: the algorithm randomly selects n fireworks positions as follows, where Sw represents the tie switch and DG represents the distributed power supply capacity. The numbers on the right represent the self-numbers of the optimization variables, and the superscripts represent the number of fireworks. In this way, each line is a firework, and each firework can be regarded as a set of input parameters for a power flow calculation.

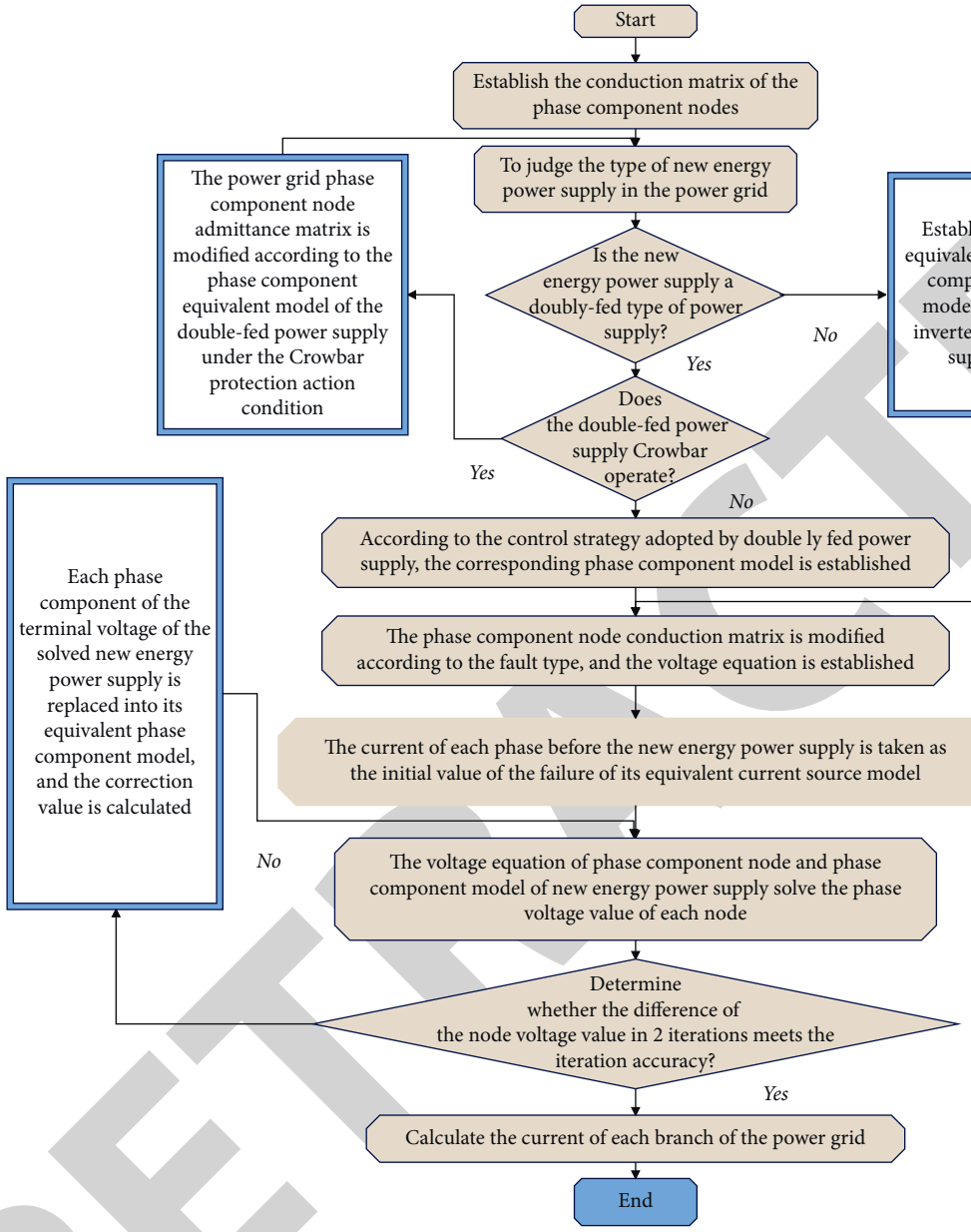

Figure 6: Flow chart of short-circuit calculation method for an unbalanced distribution network connected to NE.

$$FW = \begin{bmatrix} Sw1_1 & Sw2_1 & Sw3_1 & Sw4_1 & Sw5_1 & DG\ 1_1 & DG\ 2_1 & DG\ 3_1 \\ \vdots & & \vdots & \vdots & \vdots & \vdots & \vdots & \vdots \\ \vdots & \vdots & \vdots & \vdots & \vdots & \vdots & \vdots & v \\ Sw1_n & Sw2_n & Sw3_n & Sw4_n & Sw5_n & DG\ 1_n & DG\ 2_n & DG\ 3_n \end{bmatrix}. \tag{19}$$

In order to make the initialization of the matrix FW more convenient, and to avoid that the initialized matrix has no feasible solution, the algorithm generates the initialization matrix according to the following method [19]:

(1) The algorithm inputs the network parameter matrix (node, branch, and parameters), and generates the "pseudoring network" branch array of the input network by generating the "pseudoring network" program.

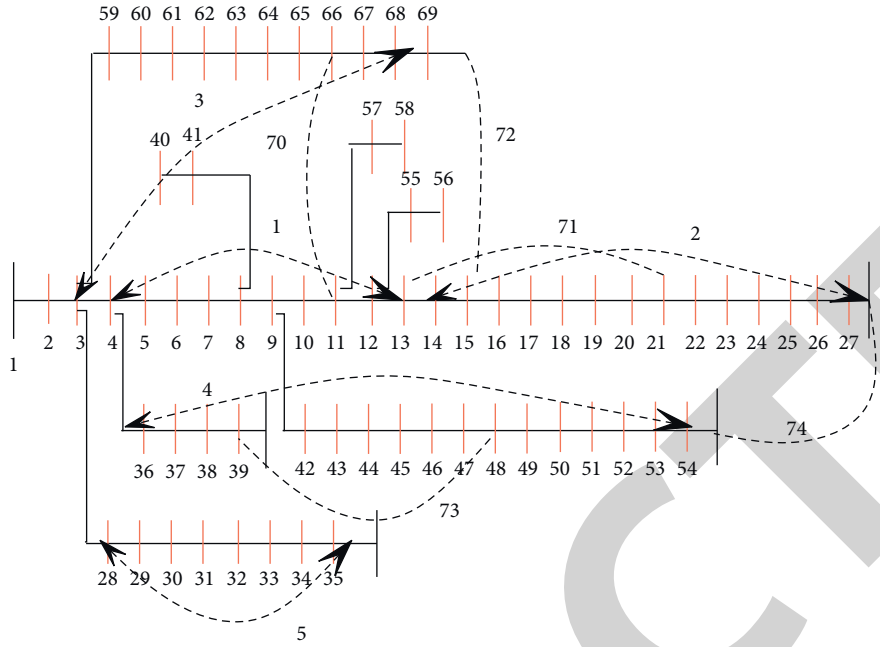

Figure 7: Test circuit.

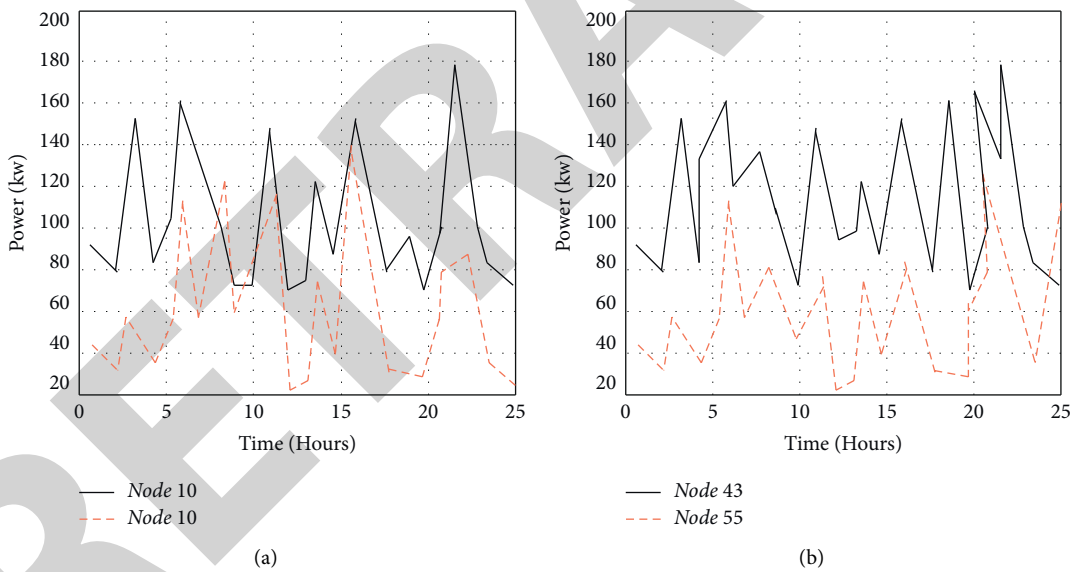

Figure 8: Wind farm output test of nodes.

(2) The algorithm selects the shutdown branch node of each "pseudoring network" in the form of random numbers, and removes the shutdown branch from the original network parameters to form a new topology structure.

(3) The algorithm passes through the ring network and island detection procedures. If the new structure does not generate ring networks and islands, the breadth-first numbering procedure is used to renumber the network nodes to form a new input network parameter matrix. If a ring network or island node is generated, the algorithm returns to step 1, and the above 3 steps are repeated.

(4) The algorithm randomly generates the capacity of the distributed power supply, forms a row vector of the matrix FW with the "pseudoring network" generated in step 3, and takes the row vector into

the power flow calculation program as an input parameter. If there is a power flow solution, the row vector is used as a row of the matrix FW.

(5) The algorithm returns to step 1 to generate the second group of fireworks, until the number of fireworks reaches twenty, and the initialization ends.

Step 3: the algorithm releases the selected n fireworks, which in the power distribution system refers to the power flow calculation based on the selected set of variables.

In the first loop, the power flow calculation is performed for each row vector in the initial matrix.

Step 4: for the calculated results of each firework, $F(xp)$.

Step 5: in the same way, the algorithm calculates the Gaussian variation factor and calculates the fitness value.

Step 6: the algorithm compares the fitness value of the objective function of all operators (fireworks, sparks, and mutation sparks) and selects the fireworks with the smallest fitness value as the fireworks of the next explosion.

Step 7: the algorithm randomly selects from them to determine other n-1 new firework positions.

Step 8: if the above cycle does not reach the set maximum number of cycles, the algorithm returns to step 3. If the maximum value of the loop is reached, the algorithm jumps out of the loop and outputs each optimized variable value of the best fitness value.

The above are the main steps of applying the fireworks algorithm to the optimization of the distribution network feeder reorganization considering the distributed power configuration problem.

3. ACS of Multiemergency Power Supply Network System Connected to NE

In the networked protection system of the distribution network, the decision-making unit of the distribution network protection center is configured to realize the function of regional protection of the distribution network [20]. The local unit is equipped with a power distribution terminal, which mainly realizes the functions of local data collection and opening and closing control of the circuit breaker. The communication system mainly realizes the information exchange function between the central decision-making unit and each local unit. Figure 4 is a schematic diagram of the networked protection system of the distribution network.

The networked protection principle of the distribution network connected to NE is shown in Figure 5.

After the NE unit is connected to the power grid, there is a nonlinear relationship between the positive and negative sequence components of the fault current fed by the unit and the node voltage at the grid connection point of the unit. Therefore, the node voltage equation of the grid phase component can be jointly constructed and the short-circuit calculation model of the phase component of different types of NE units can be iteratively solved. Figure 6 is a flow chart of multiple types of NE sources [21].

Table 1: Effect evaluation of the ACS of the multiemergency power supply networking system connected to NE.

No.	Control effect
1	86.499
2	84.927
3	82.125
4	86.334
5	86.693
6	83.077
7	82.048
8	86.815
9	88.843
10	83.409
11	87.411
12	87.640
13	82.920
14	85.048
15	84.851
16	88.715
17	84.498
18	84.286
19	84.205
20	83.260
21	85.473
22	84.466
23	87.443
24	85.220
25	86.084
26	84.943
27	88.733
28	88.070
29	84.176
30	85.112
31	83.598
32	87.937
33	87.587
34	87.886
35	88.787
36	88.261
37	83.201
38	82.922
39	85.085
40	84.813
41	84.892
42	87.818
43	85.277
44	86.965
45	82.603
46	82.338
47	84.646
48	86.326

The questions raised are tested on the PG&E69 node standard test system. In this paper, fans are configured at nodes 10, 18, 43, and 55 as shown in Figure 7.

The wind farm output test of the node is shown in Figure 8.

Based on the above analysis, the effect evaluation of the ACS of the multiemergency power supply network system connected to NE is carried out as shown in Table 1.

It can be seen from the above research that the ACS of the multiemergency power supply network system connected to NE proposed in this paper has the established effect.

4. Conclusion

As the common carrier of power transmission and power market, the power grid is the basic platform and main medium to ensure the development of NE. Therefore, the CD of NE and regional power grids is an inherent requirement and an inevitable choice to transform the energy structure and power development mode and achieve sustainable development. This paper proposes a method to optimize the distribution network feeder reorganization and distributed power configuration problems based on the fireworks algorithm to reduce the network loss and improve the voltage distribution. In addition, distribution network reorganization and distributed power configuration optimization can more effectively minimize network losses and improve voltage distribution. Through the experimental research, it can be seen that the ACS of the multiemergency power supply network system connected to NE proposed in this paper has the established effect.

Data Availability

The labeled dataset used to support the findings of this study are available from the corresponding author upon request.

Conflicts of Interest

The authors declare no conflicts of interest.

Acknowledgments

This work was supported by 2019 Inner Mongolia Autonomous Region Science and Technology Project "Research and Demonstration Application of Multi-Emergency Power Networking Technology under Disaster Conditions" (2019GG373).

References

[1] F. Xiao and Q. Ai, "Data-driven multi-hidden Markov model-based power quality disturbance prediction that incorporates weather conditions," *IEEE Transactions on Power Systems*, vol. 34, no. 1, pp. 402–412, 2019.

[2] W. Qiu, Q. Tang, J. Liu, and W. Yao, "An automatic identification framework for complex power quality disturbances based on multifusion convolutional neural network," *IEEE Transactions on Industrial Informatics*, vol. 16, no. 5, pp. 3233–3241, 2020.

[3] S. A. Kumar and D. Chandramohan, "Fault test analysis in transmission lines throughout interfering synchrophasor signals," *ICT Express*, vol. 5, no. 4, pp. 266–270, 2019.

[4] F. Z. Dekhandji, S. Talhaoui, and Y. Arkab, "Power quality detection, classification and monitoring using LABVIEW," *Algerian Journal of Signals and Systems*, vol. 4, no. 2, pp. 101–111, 2019.

[5] W. Qiu, Q. Tang, K. Zhu, W. Wang, Y. Liu, and W. Yao, "Detection of synchrophasor false data injection attack using feature interactive network," *IEEE Transactions on Smart Grid*, vol. 12, no. 1, pp. 659–670, 2021.

[6] C. Liang, Z. Teng, J. Li et al., "A Kaiser window-based S-transform for time-frequency analysis of power quality signals," *IEEE Transactions on Industrial Informatics*, vol. 18, no. 2, pp. 965–975, 2022.

[7] X. Deng, D. Bian, W. Wang et al., "Deep learning model to detect various synchrophasor data anomalies," *IET Generation, Transmission & Distribution*, vol. 14, no. 24, pp. 5739–5745, 2020.

[8] A. Sundararajan, T. Khan, A. Moghadasi, and A. I. Sarwat, "Survey on synchrophasor data quality and cybersecurity challenges, and evaluation of their interdependencies," *Journal of Modern Power Systems and Clean Energy*, vol. 7, no. 3, pp. 449–467, 2019.

[9] A. Khair, M. Zuhaib, and M. Rihan, "Effective utilization of limited channel PMUs for islanding detection in a solar PV integrated distribution system," *Journal of the Institution of Engineers: Serie Bibliographique*, vol. 102, no. 1, pp. 75–86, 2021.

[10] M. Asadi, M. N. Harikandeh, and M. Hamzenia, "Detecting and locating power quality issues by implementing wavelet transform," *International Journal of Science and Engineering Applications*, vol. 10, no. 07, pp. 96–100, 2021.

[11] W. Wang, C. Chen, W. Yao, K. Sun, W. Qiu, and Y. Liu, "Synchrophasor data compression under disturbance conditions via cross-entropy-based singular value decomposition," *IEEE Transactions on Industrial Informatics*, vol. 17, no. 4, pp. 2716–2726, 2021.

[12] S. Vlahinić, D. Franković, B. Juriša, and Z. Zbunjak, "Back up protection scheme for high impedance faults detection in transmission systems based on synchrophasor measurements," *IEEE Transactions on Smart Grid*, vol. 12, no. 2, pp. 1736–1746, 2021.

[13] B. K. Panigrahi, A. Bhuyan, J. Shukla, P. K. Ray, and S. Pati, "A comprehensive review on intelligent islanding detection techniques for renewable energy integrated power system," *International Journal of Energy Research*, vol. 45, no. 10, pp. 14085–14116, 2021.

[14] P. K. Ganivada and P. Jena, "Frequency disturbance triggered d-axis current injection scheme for islanding detection," *IEEE Transactions on Smart Grid*, vol. 11, no. 6, pp. 4587–4603, 2020.

[15] X. Xie, Y. Zhan, H. Liu, and C. Liu, "Improved synchrophasor measurement to capture sub/super-synchronous dynamics in power systems with renewable generation," *IET Renewable Power Generation*, vol. 13, no. 1, pp. 49–56, 2019.

[16] E. M. Molla, C. H. Liu, and C. C. Kuo, "Power quality improvement using microsystem technology for wind power plant," *Microsystem Technologies*, vol. 26, no. 6, pp. 1799–1811, 2020.

[17] R. M. Radhakrishnan, A. Sankar, and S. Rajan, "Synchrophasor based islanding detection for microgrids using moving window principal component analysis and extended mathematical morphology," *IET Renewable Power Generation*, vol. 14, no. 12, pp. 2089–2099, 2020.

[18] Y. Hao, M. Wang, J. H. Chow, E. Farantatos, and M. Patel, "Modelless data quality improvement of streaming synchrophasor measurements by exploiting the low-rank Hankel structure," *IEEE Transactions on Power Systems*, vol. 33, no. 6, pp. 6966–6977, 2018.

[19] W. Qiu, Q. Tang, Y. Wang, L. Zhan, Y. Liu, and W. Yao, "Multi-view convolutional neural network for data spoofing cyber-attack detection in distribution synchrophasors," *IEEE Transactions on Smart Grid*, vol. 11, no. 4, pp. 3457–3468, 2020.

[20] A. Sankar, A. Sankar, and S. R, "Synchrophasor data driven islanding detection, localization and prediction for microgrid using energy operator," *IEEE Transactions on Power Systems*, vol. 36, no. 5, pp. 4052–4065, 2021.

[21] J. Shair, X. Xie, L. Yuan, Y. Wang, and Y. Luo, "Monitoring of subsynchronous oscillation in a series-compensated wind power system using an adaptive extended Kalman filter," *IET Renewable Power Generation*, vol. 14, no. 19, pp. 4193–4203, 2021.